Journal Name

ARTICLE

Zinc oxide nanocrystals as nano-antibiotic and osteoinductive agents

Received 00th January 20xx,
Accepted 00th January 20xx

DOI: 10.1039/x0xx00000x

www.rsc.org/

Nadia Garino[a,b]†, Pasquale Sanvitale[a]†, Bianca Dumontel[a], Marco Laurenti[a], Montserrat Colilla[c,d], Isabel Izquierdo Barba[c,d], Valentina Cauda[a]*, Maria Vallet- Regi[c,d]*

The use of nanomaterials in the field of bone tissue engineering implants is continuously dealing with the development of innovative solutions to common problems, as infection by colonization with common microbial agents, antibiotic bacterial resistance, and the formation of new bone tissue. Among them, ZnO nanostructures are promising candidates thanks to their intrinsic antimicrobial activity and high biocompatibility.

In this paper we aim to analyse the behaviour of ZnO nanocrystals (ZnO NCs), prepared with a new synthetic approach and not embedded in any composite matrix, for bone implants applications in-vitro. In particular, we have developed a novel, fast and reproducible microwave-assisted synthesis, obtaining highly-crystalline, round-shaped ZnO NCs of 20 nm in diameter as an extremely-stable colloidal solution in ethanol. Part of them were also chemically functionalized by anchoring amino-propyl groups to the ZnO surface (ZnO-NH_2 NCs). Thus, the role of both ZnO NCs concentration and surface chemistry are tested in terms of biocompatibility towards pre-osteoblasts cells, promotion of cell proliferation and differentiation, and also in terms of antimicrobial activity against Gram positive and negative bacteria, such as *Escherichia coli* and *Staphylococcus aureus*, respectively. The results propose the ZnO-NH_2 NCs as the most promising candidate to solve infections disease in bone implants and promote bone tissue proliferation at the same time, even at high concentrations. Whereas further investigations are needed for example to clarify the mechanism inhibiting biofilm formation and to investigate their role in in-vivo assays, we demonstrated that a fine and reproducible control over the chemical and structural parameters in ZnO nanomaterials can open new horizons in the use of functionalized ZnO NCs as a highly biocompatible and osteoinductive nanoantibiotic agent for bone tissue engineering.

Introduction

Nowadays, infections due to both Gram positive and negative pathogens are developing an evolved resistance to conventional antibiotics, impairing the effects of these drugs and posing serious problems to public health in the long term. Bone infections related to the implantation of orthopaedic implants are also facing this important antibiotic resistance issue. In particular, during the insertion of orthopaedic implants, bacteria from patient's skin or mucosa can enter and adhere to the surface of implant and start to produce the antibiotic-resistant biofilm. This phenomenon results in osteomyelitis, localised bone destruction, prolonged hospitalisation, intense antibiotic treatment and, in the most serious cases, the replacement of the prosthesis.[1]

It is thus necessary to start exploring either new antibiotic formulations or novel inhibition pathways to solve the bacterial resistance. Unfortunately, there is no certainty about the effectiveness of new antimicrobial drugs because bacteria can develop resistance in a timely manner. A new approach to overcome this challenging and infectious disease can be the use of antimicrobial nanomaterials. At first, nanomaterials were proposed as carriers for antibiotics to improve their pharmacokinetics and accumulation, and to reduce side effects.[2, 3] A more innovative approach is the use of intrinsically-antimicrobial nanomaterials, where the antimicrobial activity is not given by the pharmaceutical effect of an antibiotic, but it directly comes from the intrinsic properties of the nanosized material.[4] To this end, several metal and metal oxide micro- and nanostructures have been proposed due to their ability to produce reactive oxygen species or dissolve in cations, both toxic for the majority of microbial cells.[5]

Among them, zinc oxide (ZnO) is one of the most promising inorganic antimicrobial material. At the bulk or micro-sized level, it shows reduced toxicity to eukaryotic cells (it is actually considered a GRAS - generally recognized as safe - substance approved by FDA[6]) and can overcome the bacterial resistance to a certain extent.[5, 7]

[a]*Department of Applied Science and Technology, Politecnico di Torino, Corso Duca degli Abruzzi 24, 10129 Turin, Italy;*
[b]*Istituto Italiano di Tecnologia, Center for Sustainable Future Technologies, Via Livorno 60, 10144 Torino, Italy*
[c]*Departamento de Química en Ciencias Farmacéuticas, Universidad Complutense de Madrid, Plaza Ramón y Cajal s/n, 28040 Madrid, Spain.*
[d]*Networking Research Center on Bioengineering, Biomaterials and Nanomedicine (CIBER-BBN), Madrid, Spain*
† These authors contributed equally

Electronic Supplementary Information (ESI) available: ZnO NCs size distribution curves in ethanol and water, Fourier Transform Infra-Red (FT-IR) spectra, Additional Fluorescent microscope images, Cell differentiation assays in term of total protein content, Cell morphology evaluation by optical microscopy. See DOI: 10.1039/x0xx00000x

The use of nanosized ZnO in biomedical applications,[8, 9] in particular in bone tissue engineering, can be envisioned owing to its excellent antimicrobial properties, its biocompatibility and partial biodegradability,[10] facile synthetic approaches in different sizes and shapes,[11] and ease functionalization procedures of the surface.[12] However, some issues are still unsolved concerning its potential toxicity to eukaryotic cells, which can impair at different dosages either healthy or tumor cells.[13, 14] Thus, the use of ZnO as a nanoantibiotic[4] requires a careful evaluation of the interactions between the nanomaterials and living cells, tissues and adjacent organs, and thus of dose administration and recalibration in the desired antimicrobial therapy.

The antibacterial activity of ZnO nanostructures is related to three main probable mechanisms:[9] (i) Reactive Oxygen Species (ROS) generation, (ii) release of Zn^{2+} cations and (iii) nanoparticle action. The ROS generation is the predominant mechanism and is promoted by the presence of crystalline defects in nano-sized ZnO structures, even in absence of any photoactivation stimulus. Due to the semiconductor band structure of ZnO, the electrons (e^-) are promoted in the conduction band, whereas unpaired holes (h^+) remain in the valence bands. The migration of both e^- and h^+ at the surface of the nanomaterials promotes their combination with water-adsorbed molecules, generating ROS, thus hydroxyl radicals, singlet oxygen and superoxide radicals. Hydroxyl radicals are the most reactive species and they can quickly interact with every type of biological molecules.

The release of Zn^{2+} ions from ZnO nanostructures, owing to their chemical instability in biological media,[10] is another important mechanism in antibacterial activity of ZnO. Zn^{2+} ions can adsorb to the negatively charged bacteria surface through electrostatic forces. This interaction leads to the loss of the charge balance and deformations of the cell occur with consequent bacteriolysis. At the same time, Zn^{2+} can penetrate the cell membrane and interact with functional groups as sulphate and phosphate groups, resulting in a structural change of proteins and provoking the destruction of bacteria by unbalanced metabolism.

Finally, the penetration of ZnO nanoparticles through the bacterial membrane and its consequent disorganisation also leads to bacterial death and thus is the third mechanism to take into account. This phenomenon is specifically due to the high specific area and surface energy of ZnO nanomaterials, able to adsorb and accumulate at the membrane and in the cytoplasm.

Despite these most probable mechanisms against bacteria, the influence of the medium components, and the different sizes and surface chemistry of ZnO nanomaterials have also to be accounted. Therefore, the real antimicrobial mechanisms are still under investigation and have to be proven depending on ZnO morphology, chemical reactivity and surface, and bacteria cell type as well.[15]

It is thus crucial to control the ZnO particles' size, morphology and surface chemistry to efficiently tune on the one hand the antibacterial properties and on the other hand the biocompatibility towards healthy cells in case of biomedical implants or drug delivery devices.[16]

Regarding specifically the use of ZnO nanomaterials for bone tissue engineering, ZnO was proposed as a suitable filler in composite matrices based on hydroxyapatite,[17, 18] graphene oxide,[19] polymers,[20, 21] or as a coating for orthopaedic and dental implants promoting antibacterial response together with osteoblast growth, adhesion and their metabolic activity.[22] Colon et al.[23] have analysed the effects of ZnO micro- and nano-powders, pressed into compacts, on the osteoblast functions and *S. epidermidis* adhesion. The results of this study provided the first evidence of significantly greater osteoblast adhesion, alkaline phosphatase (ALP) activity, and calcium mineral deposition on nanophase ZnO with respect to the microphase counterpart, as well as a reduction of *S. epidermidis* adhesion. Moreover, it was reported that an appropriate concentration of zinc ions could enhance osteoblast cell proliferation and differentiation,[24] promoting ALP activity and osteocalcin (OCN) secretion, which are considered an early marker and a major marker of osteoblast differentiation at the late stage, respectively.[25]

The aim of this paper is to analyse the behaviour of ZnO nanocrystals (ZnO NCs), not embedded in any composite matrix, for bone implants applications in-vitro. We have developed a novel microwave-assisted synthesis to obtain the ZnO NCs in a fast, highly-reproducible and efficient way. Such NCs, having 20 nm in diameter and a high degree of crystallinity, are also chemically functionalized with amine groups, in order to investigate in-vitro the effect of their surface chemistry and charge.

Thus, the role of ZnO NCs concentration and functionalization is tested both in terms of biocompatibility related to pre-osteoblasts cells, promotion of cell proliferation and differentiation, and also in terms of antimicrobial activity against Gram positive and negative bacteria, such as *Escherichia coli* and *Staphylococcus aureus*. The results show a promising behaviour of amine-functionalized ZnO NCs for bone tissue engineering, even at high concentrations, leading to promoted osteogenic behaviour and high antimicrobial activity. It is thus demonstrated that a fine control over the chemical and structural parameters in ZnO nanomaterials can open new horizons in the use of functionalized ZnO NCs as a highly biocompatible nanoantibiotic for bone tissue engineering.

Results and discussion

We developed for this work a novel wet-chemical synthetic approach to obtain tiny and homogeneous ZnO NCs. The used approach involves a fast, highly-reproducible and efficient microwave-assisted synthesis method,[26] hydrolysing the zinc acetate dehydrate precursor in a polar solvent (methanol) in presence of potassium hydroxide. The microwave-assisted solvothermal synthesis shows various advantages with respect to conventional synthetic procedures. In fact, due to a rapid and homogeneous heating it is possible to guarantee very fast kinetic rates and short reaction times, low energy consumption and simultaneous nucleation of nanocrystals that lead to obtain a uniform and reproducible dimensional range.[27]

Thanks to this process, highly-dispersed, round-shaped nanocrystals as an extremely-stable colloidal solution in ethanol and water were finally obtained. Part of them were also chemically modified by anchoring amino-propyl groups to the ZnO surface, as previously reported by some of us.[10, 28, 29] The produced nanomaterials were then characterized as described below.

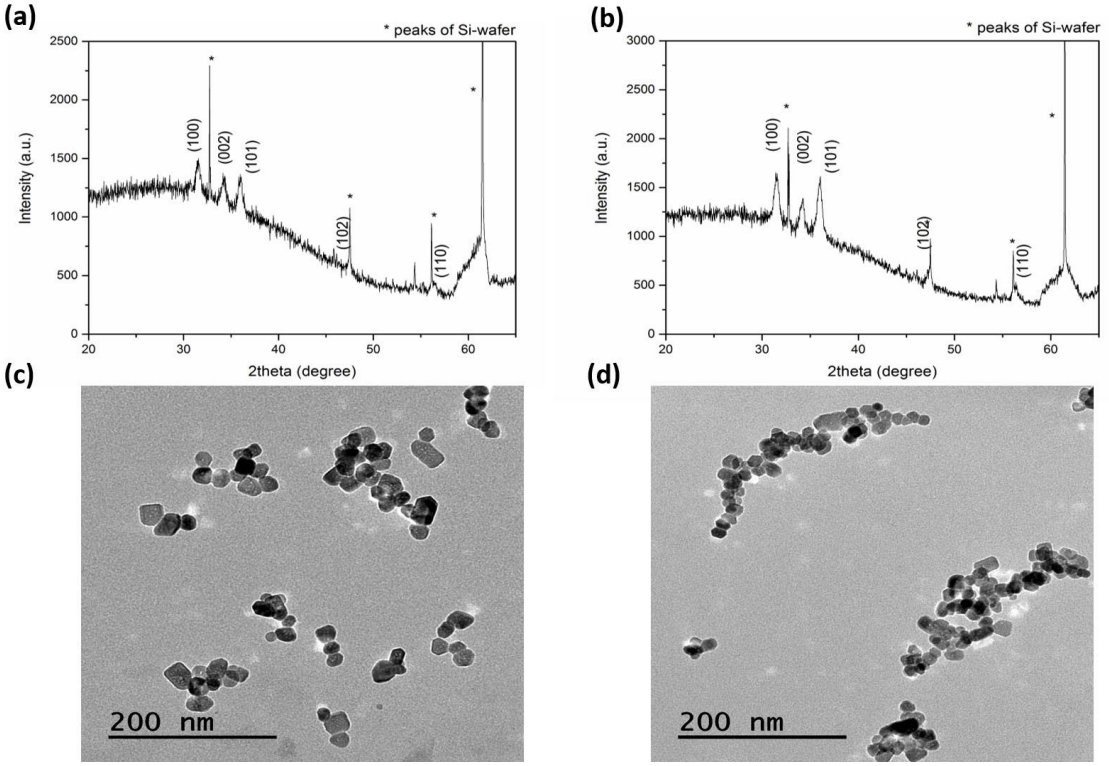

Figure 1. Structural and morphological characterization: XRD patterns for (a) ZnO and (b) ZnO-NH_2 NCs; TEM micrographs of (c) ZnO and (d) ZnO-NH_2 NCs.

Morphological and structural characterization of the ZnO NCs

X-Ray Diffraction (XRD) was performed in order to obtain information about phase identification, along with phase quantification, percentage of crystallinity, crystallite size and unit cell size. Figures 1a and 1b show the XRD patterns of pristine ZnO NCs and ZnO-NH_2 NCs. The comparison of patterns with data bank (JCPDS 36-1451) has confirmed the crystalline structure of the particles. In particular, the peaks at 31.9°, 34.4°, 36.4°, 47.6°, 56.7° are indexed to (100), (002), (101), (102) and (110) planes, respectively. These correspond to the Miller indexes of hexagonal wurtzite structure of ZnO, according to the literature[30, 31] and compared with the standard reference pattern of ZnO. It is also clear that the chemical functionalization has not altered the crystalline structure of ZnO. By using the Debye-Scherrer formula and considering the dominant peaks, it was possible to estimate the dimension of crystallites, resulting to be around 15 nm for both pristine and functionalized ZnO NCs.

Transmission Electron Microscopy (TEM) studies confirmed these results and allowed to obtain additional information about the particle's morphology and size (Figures 1c and 1d), showing similar polygonal shape, typical of ZnO NCs in both cases. The stability behaviour of ZnO NCs show highly monodispersed particles sizes for both pristine and amine-functionalized ZnO NCs in both ethanol and water media, as reported by the Dynamic Light Scattering measurements in Figures S1 of the Supporting Information (S.I.). Fourier-Transform Infrared (FTIR) spectra of both ZnO and ZnO-NH_2 NCs show some common features between the two different samples, but in the case of ZnO-NH_2 NCs the presence of typical vibration modes associated to functional groups present in the 3-aminopropyltrimethoxysilane molecule (APTMS) confirms the successful functionalization of the ZnO surface (Figure S2 in the S.I.).

Journal Name

ARTICLE

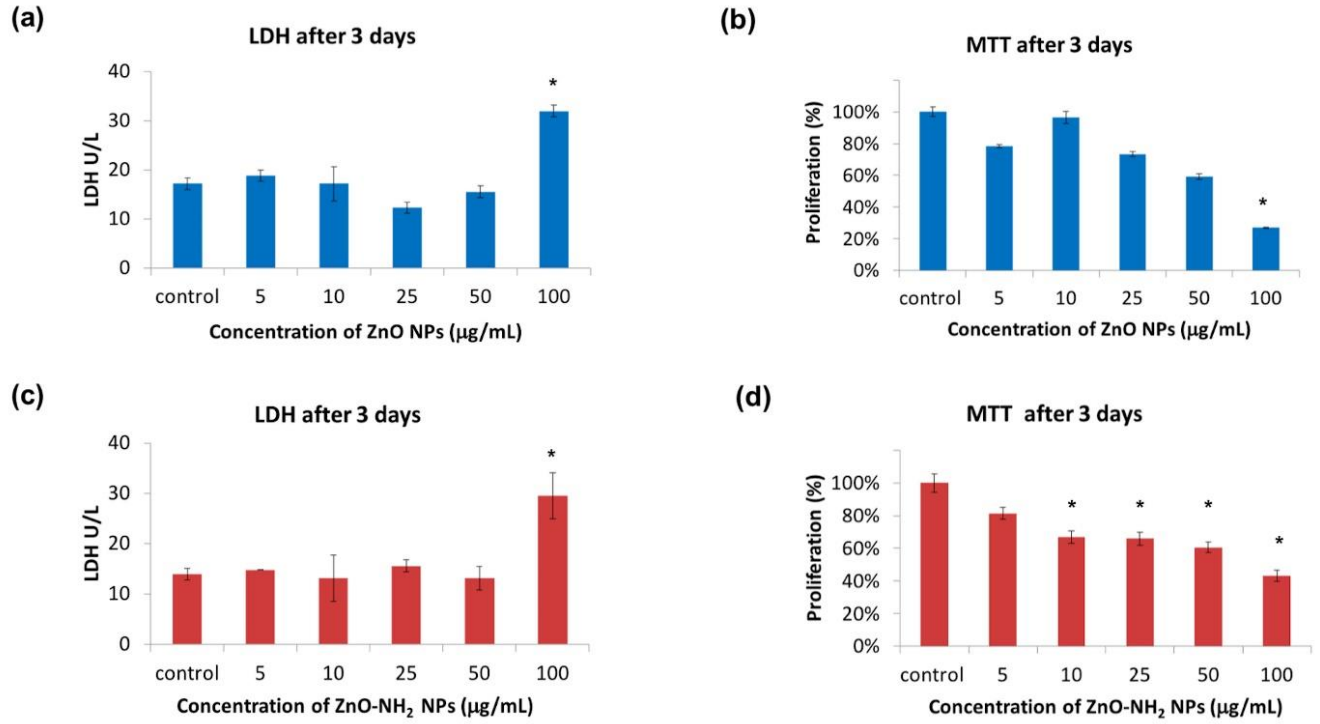

Figure 2. In-vitro biocompatibility assays: cytotoxicity by LDH released into the medium after 3 days of incubation with different concentrations of (a) ZnO and (c) ZnO-NH_2 NCs. Proliferation results in terms of mitochondrial activity (MTT) after 3 days of incubation and with different concentrations of (b) ZnO and (d) ZnO-NH_2 NCs ($p < 0.05$, significant differences compared to control are denoted by an asterisk (*))

Biocompatibility studies

The biocompatible or cytotoxic behaviours of both pristine and functionalized ZnO NCs at different concentrations were monitored in living pre-osteoblast cells from mouse calvaria. Both lactate dehydrogenase (LDH) production and the mitochondrial activity (MTT) were recorded after 3 days of cell incubation with the nanocrystals with and without functionalization and at different concentrations, to give a complete picture of the cytotoxicity and the cell proliferation behaviour. LDH is an enzyme released by cells in case of cell membrane rupture, thus indicating a cytotoxic effect. Interestingly, the LDH tests reported in Figures 2a and 2c for both pristine and functionalized ZnO NCs, respectively, evidenced no cytotoxic effect in both cases up to the concentration of 50 µg/mL of NCs. Actually, no significant differences were registered in comparison with the control test. In contrast, the concentration of 100 µg/mL of both pristine ZnO NCs and ZnO-NH_2 NCs exhibited a cytotoxic effect on pre-osteoblast cells, displaying a double quantity of LDH produced with respect to the control.

The MTT proliferation test is based on the ability of mitochondrial enzymes to reduce the MTT molecule to formazan. This measurement is commonly related with the cell viability and cell proliferation as previously reported in the literature.[32] According to Figures 2b and 2d, both pristine and functionalized ZnO NCs showed an adequate cell proliferation up to a certain concentration: in general, a decrease of mitochondrial activity occurred by increasing the concentration of NCs with respect to the control without nanocrystals. The proliferation ranges from 90% to 70% up to the concentration of 25 µg/mL (compared to control), then a slight decrease occurs for 50 µg/mL (≈60%) both for pristine and functionalized NCs. Regarding the highest concentration of 100 µg/mL, there is a significant reduction of the proliferation down to 27% for ZnO NCs and 43% for ZnO-NH_2 NCs compared to the control. These results are in line with the LDH test. Therefore, both LDH and MTT assays has highlighted the great biocompatibility of ZnO and ZnO-NH_2 up to the concentration of 50 µg/mL. On the other side, the concentration of 100 µg/mL has shown a cytotoxic activity and inhibited the cell proliferation. This cytotoxic effect is generally reported in the

literature[10, 26] as an intracellular release of cytotoxic Zn^{2+} cations due to ZnO dissolution, or as a consequence of an oxidative stress by Reactive Oxygen Species, due to the ZnO present intracellularly.[33]

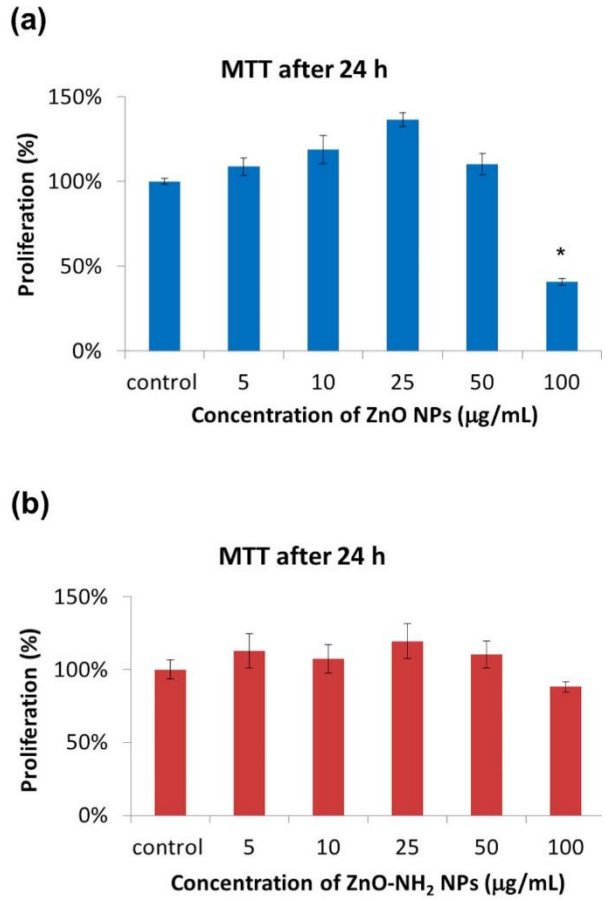

Figure 3. Proliferation results in terms of MTT of MC3T3-E1 (at 70% of confluence) and incubated for 1 day with different concentrations of (a) ZnO and (b) ZnO-NH_2 NCs ($p < 0.05$, significant differences compared to control denoted by an asterisk (*))

In order to have further information on biocompatibility behaviour another assay was performed. The cells were cultured up to the 70% of confluence and then treated with the nanocrystals (at different concentrations and with or without functionalization). This procedure was necessary to simulate the interaction between a pre-formed bone tissue and antibacterial agents, in order to analyse how they may affect the viability of the tissue. In this case, the proliferation via MTT was measured after 24 h of incubation (Figure 3) and the cell morphology was studied under fluorescent microscope after 4 days of incubation (Figure 4). The values of MTT tests are of the same order of the control up to a concentration of 50 μg/mL for pristine ZnO NCs. Actually, the mitochondrial activity is around 100% or higher compared to the control, with a peak of mitochondrial activity for the concentration of 25 μg/mL, where the proliferation is increased up to 130%. Unfortunately, a significant decrease occurs in correspondence of the highest concentration (100 μg/mL), where mitochondrial activity drops down to 41%. These results are indeed comparable to what reported in Figure 2, showing again a concentration-dependence biocompatibility of the ZnO NCs.

The results about ZnO-NH_2 are similar with just few differences. The best proliferation value is obtained for the concentration of 25 μg/mL, but the peak is less pronounced. Interestingly, the concentration of 100 μg/mL does not show significant differences and the mitochondrial activity is still close to control. This result highlights the first difference between pristine and functionalized ZnO NCs.

Confocal microscope images give further information and permit to investigate the cell morphology after ZnO NCs incubation. Actin was stained with Atto565-conjugated phalloidin (red) and nuclei stained with DAPI (blue). Figure 4 shows the typical well-spread morphology of osteoblasts after incubation with ZnO NCs at 25 μg/mL. In addition, further images at the other concentrations are reported Figures S3 and S4 in the S.I. Note that there is a slight increase of the number of the cell after incubation with the nanoparticules at 25 μg/mL, which is confirmed by an increase in the cellular thickness from 73±10 μm for the control to 123 ±15 μm in presence of ZnO NCs. On the contrary, at higher concentration of pristine ZnO NCs (100 μg/mL), the cells exhibit a spherical morphology, non-defined actin filaments and reduced confluence, meaning a clear cytotoxic effect at this concentration. These results have confirmed the previous ones, evidencing a good biocompatibility of ZnO NCs up to 50 μg/mL.[7]

Regarding the functionalized ZnO-NH_2 NCs, this cytotoxic effect is less noticeable, because the cells in contact with 100 μg/mL show a well-spread morphology, still fluorescent actin filaments, but the grade of confluence is sensibly inferior compared to the control cells. ZnO-NH_2 is again confirmed to be more biocompatible, especially for the highest sample concentration of 100 μg/mL in these experimental conditions.

Differentiation assay: ALP

Differentiation is a process by which unspecialized cells, pre-osteoblasts, become specialized cells with the function to restore the bone. For this purpose, the activity of ALP (alkaline phosphatase), a marker enzyme for determining osteoblasts phenotype was monitored. In particular, the ALP activity of both kinds of ZnO NCs was determined after 10 days of incubation in pre-osteoblast cells. In Figure 5a it is possible to observe a progressive decrease of ALP activity by increasing the concentration of ZnO NCs, and even in this case the lowest value is for 100 μg/mL. Regarding the total protein content (Figure S5 top in the S.I.), the trend is very similar to the ALP activity. No significant differences are observed up to a concentration of 10 μg/mL, while there is a drop from 25 μg/mL to higher concentration values. On the other side, the ZnO-NH_2 NCs have shown a different behaviour. As it can be observed in Figure 5b, there are no significant differences compared to the control for the ALP activity, evidencing there is no apparent inhibition at the lower concentrations of nanoparticles (below 100 μg/mL). At the highest concentration of 100 μg/mL, around 20% decrease of the ALP activity is obtained. A similar trend is observed for the total protein content in Figure S5 bottom of the S.I.

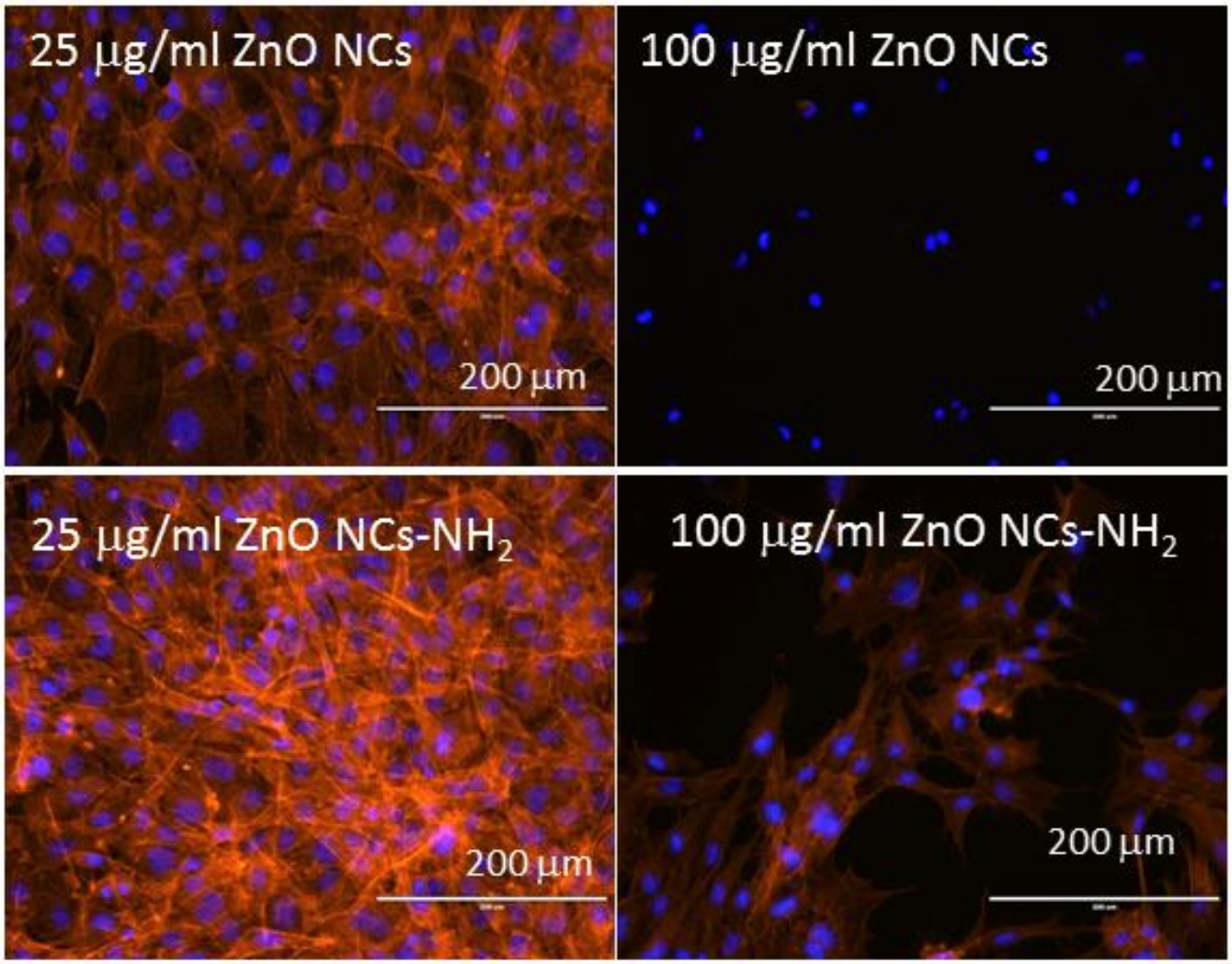

Figure 4. Confocal Microscopy images of pre-osteoblasts cultured up to 70% of confluence after incubation for 4 days with ZnO and ZnO-NH_2 NCs at different concentrations. All confocal images have been obtained n the same conditions and are the Z projection of different images taken at different depths.

The cell morphology in bright field at optical microscope was also recorded at every concentration, both for the pristine and functionalized incubated NCs (see Figures S6 and S7 in the S.I.). MC3T3-E1 cells exhibit a well spread morphology, with a high degree of confluence, up to the concentration of 50 µg/mL for pristine ZnO NCs. As observed above, the cells treated with 100 µg/mL of ZnO NCs present a spherical morphology, indicating cell sufferance and death, with a minor grade of confluence.

Regarding the cells treated with ZnO-NH_2 NCs for ten days at different concentrations, in all cases a well-spread morphology of MC3T3-E1 cells is observed, including the highest concentration of 100 µg/mL for ZnO-NH_2 NPs. We can observe a slightly lower confluence for the most concentrated sample with respect to the other ones. However, these optical microscope images have confirmed the results of ALP activity and total protein content, showing the prominent biocompatible and osteoinductive role, even at high concentrations, of the ZnO-NH_2 NCs.

Antimicrobial activity

The antimicrobial activity of different NCs was determined against Gram positive (*S. aureus*) and Gram negative (*E. coli*) bacteria in planktonic stage, after 24h of incubation at different concentration. Figure 6 summarizes these results in terms of logarithmic scale of CFU quantification. The obtained results show a remarkable antimicrobial effect in the antimicrobial activity in both pristine ZnO and functionalized ZnO-NH_2 NCs against two bacteria for all bacteria. However, there is notable differences between both strains. Regarding the antimicrobial activity against *E. coli*, it is very interesting to notice that The results highlight particularly that there is no effect of NCs concentration, each one showing a 100% reduction of bacteria viability. The same behaviour was observed both for pristine and functionalized nanocrystals. On the other side, the activity against *S. aureus* was slightly different.

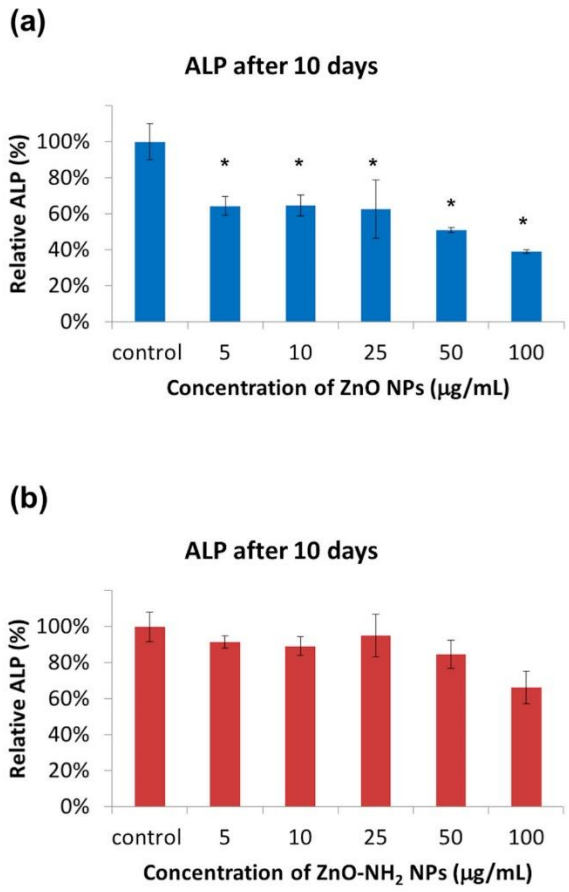

Figure 5. Differentiation assays in term of ALP after 10 days of incubation with (a) ZnO and (b) ZnO-NH_2 NCs at different concentrations. ($p < 0.05$, significant differences compared to control denoted by an asterisk (*))

The peak of antimicrobial activity is obtained for the concentration of 25 µg/mL for both ZnO and ZnO-NH_2 NCs, showing a reduction in viability around 99.98 and 99.99% (less than 100 CFU/mL), respectively. In contrast, the antimicrobial activity is reduced at higher concentration, in particular for the concentration of 50 µg/mL of ZnO-NH_2 NCs, resulting in only 99.85% of bacteria inactivation (in this case the concentration is higher of 10^2 CFU/mL, which could considered not effective. This performance can be explained by the aggregation of nanocrystals when dispersed in PBS, as previously observed by some of us.[31] In fact, by increasing the concentration, there is a greater probability to form huge aggregates, which means a lower surface area to volume ratio, and thus a reduced contact with the *S. aureus* population. This behaviour was not detected with *E. coli* probably because of the different shape and resistance. In fact, *E. coli* exhibits an elongated shape while *S. aureus* a round shape, thus aggregated NCs have a major probability to get in contact with *E. coli*. In addition, *S. aureus* is a more resistant and pathogenic bacteria compared to *E. coli*. For further information, Table S1 summarizes the reduction in bacteria viability.

Journal Name

ARTICLE

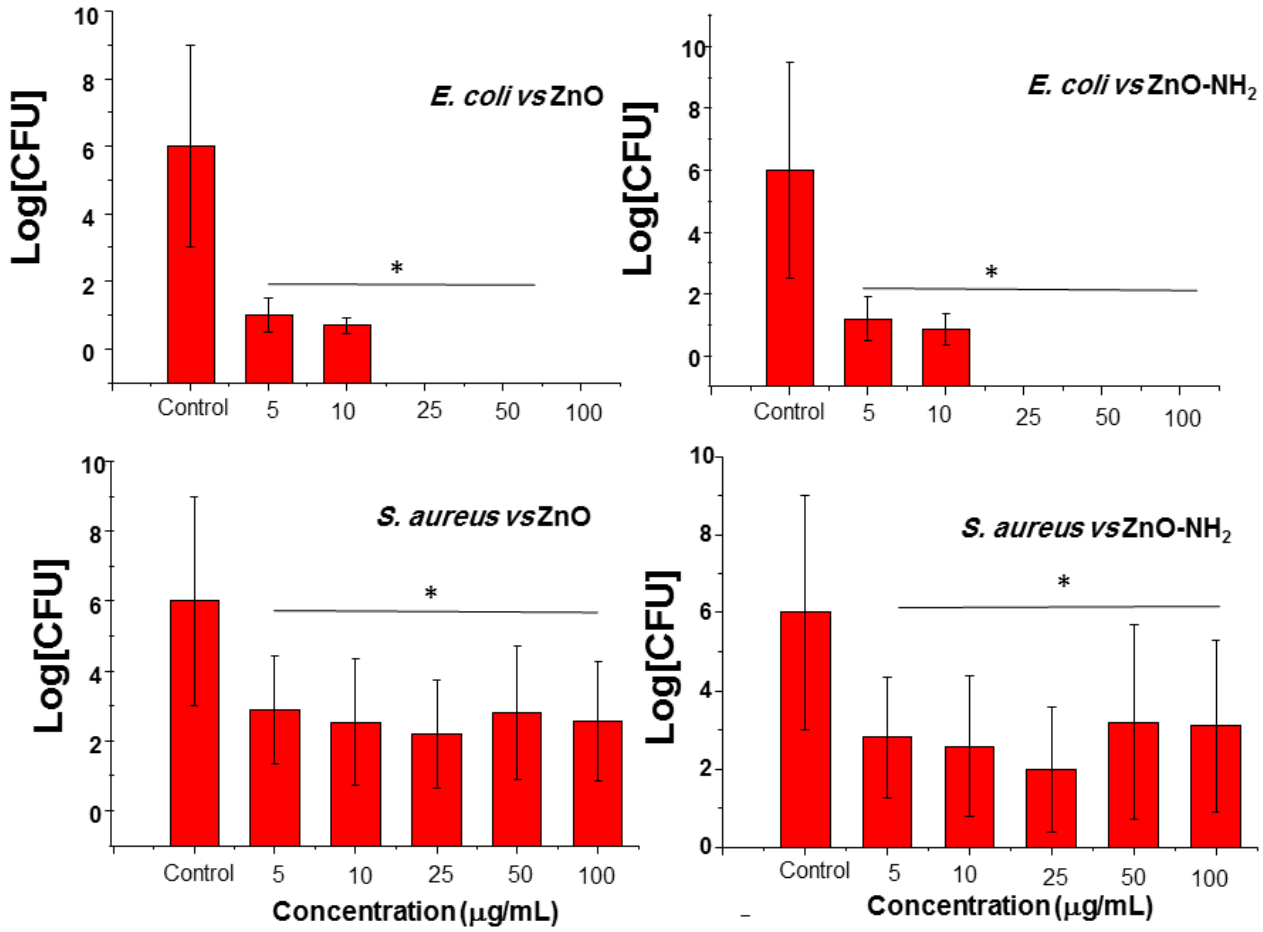

Figure 6. Logarithmic scale of CFU per mL of *E. coli* and *S. aureus* in planktonic stage incubated for 24 h in the presence of different concentrations of ZnO and ZnO-NH_2 NCs. ($p < 0.05$, significant differences compared to control denoted by an asterisk (*) in absolute value).

Experimental

ZnO synthesis and functionalization

ZnO NCs were synthesized through a novel microwave-assisted synthesis approach by using as precursors zinc acetate di-hydrate (0.1 M) and potassium hydroxide (0.2 M) (both from Sigma Aldrich) dispersed in methanol as solvent. The solution containing the zinc precursor was prepared and stirred directly in the reactor vessel. In order to initiate the zinc oxide nucleation, 0.48 µl of double-distilled water were added and then the KOH solution was mixed together in the reactor vessel. The resulting solution was put into microwave oven for 30 minutes under control of pressure at temperature of 60 °C. After this time, the colloidal solution was collected and centrifuged for 10 minutes at 5000 rpm (3500 rcf), in order to separate the methanol and reaction residuals from the newly-formed ZnO NCs. The surfactant was then removed and the precipitate was dispersed and washed in 15 mL of ethanol for two times. The as-obtained ZnO NCs pellet was suspended in fresh ethanol to give the final colloidal suspension.

The functionalization step of ZnO NCs with amino groups (NH_2) was obtained combining nanocrystals with 3-aminopropyltrimethoxysilane, (APTMS, 97%, Sigma) as already reported in [10]. More in details, 100 mg (1.23 mmol) of ZnO NCs, dispersed in ethanol, were heated to 80 °C in a 100 mL round glass flask under continuous stirring and nitrogen gas flow. 15 minutes later, 21.4 µL of APTMS (0.123 mmol, 22.05 mg, corresponding to 10 mol% of total ZnO amount) was added to the solution. The obtained mixture was refluxed under a nitrogen gas flow for 6 h and successively washed two times by separating the NCs under centrifugation (10 min, 10,000 rpm) to remove the unbound APTMS molecules.

Characterization

The ZnO NCs obtained from microwave-assisted synthesis were characterized by comparing data from different batches in order to confirm the synthesis' repeatability. In particular, the samples were analyzed by XRD (X-Ray Diffraction) in order to investigate the crystalline structure. A Panalytical X'Pert diffractometer in configuration 0-2θ Bragg-Brentano was employed. This instrument uses a source of radiation Cu-Kα (λ=1.54 Å, 40 kV e 30 mA). The samples were prepared by depositing the colloidal solution drop by drop on a silicon wafer, in order to have a sufficiently thick layer of nanocrystals. The XRD analysis was carried out with step size of 0.02° (2θ), 2θ range of 20°–70° and with an acquisition time of 100 s.

Transmission Electron Microscopy (TEM) characterization was also used to assess the morphology, size, shape and crystallinity of the nanocrystals. The samples were diluted in ultra-pure ethanol (99 %) up to a concentration of 200 µg/mL and then one drop was deposited on a copper grid with carbon mesh for HR-TEM analysis. The measurements were performed with JEM 2100HT (JEOL) multipurpose analytical HR-TEM, with an accelerating voltage of 200 kV and point resolution of 0.25 nm. HR-TEM images were acquired using a charge coupled device (CCD) camera.

Cell culture conditions

MC3T3-E1, pre-osteoblasts cells from mouse calvaria were used. Cells were grown in complete Dulbecco's Modified Eagle's Medium (α-DMEM, Sigma Chemical Company, St. Louis, MO, USA) supplemented with 2 mM L-glutamine (BioWhittaker), 100 µg·mL^{-1} penicillin (BioWhittaker), 100 g·mL^{-1} streptomycin (BioWhittaker) and fetal bovine serum (FBS, Gibco) at 10% at 37 °C under atmosphere conditions of 95% humidity and 5% CO_2. Medium was changed every day until confluence reached ≈ 90% in a P75 flask. Then cultures were trypsinized with a solution of 0.05% (w/v) trypsin and 0.02% (w/v) EDTA in sterile phosphate buffered saline (Sigma Aldrich) and counted with a Neubauer Hemocytometer. Cells were then centrifuged at 310 g for 10 min and suspended in fresh medium at a density of 2·104 cells/mL

In cellular assays the behavior of both ZnO pristine and ZnO-NH_2 NCs was studied at the following concentrations: 5 µg/mL, 10 µg/mL, 25 µg/mL, 50 µg/mL, 100 µg/mL. The desired amount of NCs was taken away from the stock solutions in ethanol, centrifuged to pellet the NCs and discard the ethanol, and then the NCs were dispersed in the final volume of cell culture medium. ZnO-free suspensions were used as control. In addition, two different experiments were performed. In the first one, cells and ZnO nanostructure were put in contact at the same time, to analyze the situation when stem cells and antimicrobial agents arrive simultaneously. In the second assay, cells were cultured up to the 70% of confluence, and then the nanocrystals were added. This procedure simulates the interaction between a pre-formed bone tissue and antibacterial agents, in order to analyse how they may affect the viability of the tissue.

Citotoxicity test – LDH

LDH activity was determined in the culture medium in contact with nanocrystals after 3 days of incubation. Activity of LDH released by the MC3T3- E1 cells is directly related to the rupture of the plasmatic membrane (cell death) that, when broken, releases all organelles and enzymes present in the cytoplasm. For this purpose, 0.750 mL of cell suspensions with a concentration of 1.33 x 10 4 cells/mL and 0.250 mL of NCs suspensions with the desired concentration were added in each plate. After adding NCs in the cells suspensions, the well plates were left in incubation under CO_2 (5%) atmosphere at 37 ℃ for 3 days. Measurements were performed by using a commercial kit (Spinreact) having an absorbance at 340 nm with a UV–Visible spectrophotometer. Two replicated were done for each concentration.

Mitochondrial activity – MTT

For evaluating cell mitochondrial activity of living cells on the different plates as well as its surroundings after 1 and 3 days of incubation, the MTT method was employed. This method is based in the reduction of 3-(4,5-dimethylazol-2-yl)-2,5-diphenyltetrazolium (yellow) to blue formazan. This measurement was used in terms of cell proliferation. For this purpose, 0.750 mL of MC3T3-E1 cells in a concentration of 104 cells/mL in complete medium were cultured in 24-well plates in presence of 0.250 ml of ZnO or ZnO-NH_2 NCs suspension at different concentrations and incubated in 5% CO_2 atmosphere at 37℃ for 3 days. This test was replicated for pre-formed bone tissue where NCs were incubated for 1 day with cells at 70% of confluence. After this time, the culture medium was substituted with 1 mL of α-MEM and 125 µL of MTT solution (5 mg/mL in PBS 1x) was added. Samples were incubated for 4 h at 37 ℃ and 5% CO_2 in dark conditions. Then, medium was removed and 500 µl of HCl-isopropanol solution 0.4 M was added. At the end, the absorbance at 570 nm was measured. Two replicates were done for each concentration.

Cell morphology studies

The morphology of pre-osteoblast cells MC3T3-E1 was studied in AMG EVOS fl LED Fluorescent Microscope. For this purpose, cells were cultured up to 70% of confluence, and then the medium was taken off. Afterwards 0.750 mL of complete α-MEM and 0.250 mL of NCs suspensions with the desired concentration were added in each plate. Samples were incubated for 4 days. After this time, adherent cells were fixed

with Paraformaldehyde (4% in PBS) for 30 minutes. Then Atto 565-conjugated phalloidin and DAPI were added in each plate to stain respectively cell actin in red and cell nuclei in blue.

Differentiation assay: Alkaline phosphatase activity – ALP

For evaluating the differentiation of MC3T3-E1, ALP measurements were employed. Alkaline phosphatase is an enzyme present in most of the organisms, with high quantities in bone, liver, placenta, intestine and kidney. ALP of the cells growing in contact with ZnO nanostructures was utilized as marker of cellular differentiation in the evaluation of the phenotype expression of osteoblasts.

For this purpose, MTC3T3-E1 pre-osteoblastic cells (104 cells/mL) were cultured directly in a 24-well plate and incubated for 10 days in contact with ZnO and ZnO-NH_2 under standard culture conditions (37 °C, 5% CO_2) using α-MEM completed medium supplemented with b-glycerolphosphate (50 mg/mL) and L-ascorbic acid (10 mM). In particular, 0.750 mL of cells suspensions with a concentration of 1.33 x 10^4 cells/mL and 0.250 mL of NCs suspensions with the desired concentration were added in each plate. Two replicates were done for each samples in two independent assays (n=4).

After incubation for 10 days, the medium was taken off and every well plate was washed twice with PBS (pH 7.4). Successively, samples were frozen and before the measurement they were frozen and unfrozen for 3 times in order to break the cell membrane and release ALP. ALP was measured employing the Spinreact kit.

CFU counting method

To examine the bactericidal effect of ZnO NCs on bacteria, in planktonic stage, direct incubation with bacteria soalution in PBS was carried out. Both *E. coli* 25922 and *S. aureus* ATCC29213 (methicillin-sensitive) have been used. In this case, the concentrations of 5 μg/mL, 10 μg/mL, 25 μg/mL, 50 μg/mL, 100 μg/mL were used in order to determine their effectivity. For this purposes 0.750 mL of bacteria suspensions in PBS with a concentration of 1.33 x 10^6 bacteria/mL and 0.250 mL of NCs suspensions with the desired concentration were added in each well of a 24-well plate. Then, NCs and bacteria suspensions were incubated for 24 h under orbital stirring at 37 °C. Two different experiments were performed for triplicated. The quantification of lived bacteria was determined by CFUs in agar. In order to be more accurate original solution and different dilutions (1/10, 1/100 and 1/1000 dilutions) were done. Thus, 20 μL of such solutions was seeded onto trypsin soy agar (TSA), incubated at 37 ºC overnight and subsequently the number of CFUs was counted. Positive controls containing bacteria was also performed and the experiments were performed in triplicate.

Statistical analysis

Data are expressed as average/mean ± standard deviation in two experiments. The software Statistical Package for the Social Sciences (SPSS) version 11.5 was used to perform statistical analysis. the variance analysis (ANOVA) was utilized for Statistical comparatives. Scheff proof was used for the post hoc evaluation of the differences among groups. In all statistical evaluations, $p < 0.05$ was considered as statistically significant.

Conclusions

In this work, uniform and highly crystalline ZnO nanoparticles were synthesized by an innovative microwave-assisted solvothermal synthesis to obtain nanocrystals of 20 nm in diameter. The results have highlighted that ZnO NCs show a great biocompatibility, towards pre-osteoblast cells and a promising antimicrobial activity against *E. coli* and *S. aureus*. Moreover, the biocompatibility and antibacterial assays performed on the functionalized ZnO-NH_2 NCs also demonstrated that a fine control over the ZnO chemical surface by amine-functionalization further improve both biocompatibility in terms of cell differentiation and proliferation and their antimicrobial capability. These findings open new horizons in the use of ZnO NCs as a highly biocompatible nanoantibiotic for bone tissue engineering.

Conflicts of interest

The authors declare no conflict of interest.

Author Contributions

The manuscript was written through contributions of all authors. All authors have given approval to the final version of the manuscript.

Acknowledgements

Part of this work has received funding from the European Research Council (ERC) under the European Union's Horizon 2020 research and innovation programme (grant agreement No 678151 – Project Acronym "TROJANANOHORSE" – ERC Starting Grant and grant agreement No 694160 – Project Acronym "VERDI"– ERC Advanced Grant). Moreover, this work has been also supported by grant MAT2015-64831-R from MINECO, Spain.

References

1. D. Campoccia, L. Montanaro and C. R. Arciola, *Biomaterials*, 2006, **27**, 2331-2339.
2. V. Cauda, B. Onida, B. Platschek, L. Muhlstein and T. Bein, *J. Mater. Chem.*, 2008, **18**, 5888-5899.
3. B. González, M. Colilla, J. Díez, D. Pedraza, M. Guembe, I. Izquierdo-Barba and M. Vallet-Regí, *Acta Biomater.*, 2018, **68**, 261-271.
4. A. J. Huh and Y. J. Kwon, *J. Controlled Release*, 2011, **156**, 128-145.
5. l. Wang, C. Hu and L. Shao, *Int. J. Nanomed.*, 2017, **12**, 1227–1249.
6. https://www.accessdata.fda.gov/scripts/cdrh/cfdocs/cfcfr/CFRSearch.cfm?fr=182.8991, (accessed 2nd July 2018).

7. M. Carmona, Y. Gun´ko and M. Vallet-Regí, *Nanomaterials*, 2018, **8**, 268.
8. Z. Ping, W. Zhengyang, L. Xia, L. Xiangmei, W. Shuilin, Y. K. W. K., W. Xianbao, C. Zhenduo, Y. Xianjin and C. P. K., *Adv. Mater. Interf.*, 2016, **3**, 1500494.
9. L. Racca, M. Canta, B. Dumontel, A. Ancona, T. Limongi, N. Garino, M. Laurenti, G. Canavese and V. Cauda, in *Smart Nanoparticles for Biomedicine*, ed. G. Ciofani, Elsevier, 2018, DOI: https://doi.org/10.1016/B978-0-12-814156-4.00012-4, pp. 171-187.
10. B. Dumontel, M. Canta, H. Engelke, A. Chiodoni, L. Racca, A. Ancona, T. Limongi, G. Canavese and V. Cauda, *J. Mater. Chem. B*, 2017, **5**, 8799-8813.
11. V. Cauda, R. Gazia, S. Porro, S. Stassi, G. Canavese, I. Roppolo and A. Chiolerio, in *Handbook of Nanomaterials Properties*, eds. B. Bhushan, D. Luo, S. R. Schricker, W. Sigmund and S. Zauscher, Springer, 2014, vol. 2014, ch. 5, pp. 137-177.
12. M. Laurenti, S. Stassi, G. Canavese and V. Cauda, *Adv. Mater. Interf.*, 2017, **4**, 1600758.
13. S. Nair, A. Sasidharan, V. V. Divya Rani, D. Menon, S. Nair, K. Manzoor and S. Raina, *J. Mater. Sci.: Mater. Med.*, 2008, **20**, 235.
14. J. W. Rasmussen, E. Martinez, P. Louka and D. G. Wingett, *Expert Opin. Drug Delivery*, 2010, **7**, 1063-1077.
15. S. Amna, M. Shahrom, S. Azman, N. H. M. Kaus, A. Ling Chuo, B. Siti Khadijah Mohd, H. Habsah and M. Dasmawati, *Nano-Micro Lett.*, 2015, **7**.
16. M. Laurenti and V. Cauda, *Materials*, 2018, **11**, 314.
17. L. Grenho, F. J. Monteiro and M. P. Ferraz, *J. Biomed. Mater. Res., Part A*, 2014, **102**, 3726-3733.
18. L. Grenho, C. L. Salgado, M. H. Fernandes, F. J. Monteiro and M. P. Ferraz, *Nanotechnology*, 2015, **26**, 315101.
19. J. Chen, X. Zhang, H. Cai, Z. Chen, T. Wang, L. Jia, J. Wang, Q. Wan and X. Pei, *Colloids Surf., B*, 2016, **147**, 397-407.
20. Y. Li, L. Sun and T. J. Webster, *J. Biomed. Nanotechnol.*, 2018, **14**, 536-545.
21. A. Bhowmick, S. L. Banerjee, N. Pramanik, P. Jana, T. Mitra, A. Gnanamani, M. Das and P. P. Kundu, *Int. J. Biol. Macromol.*, 2018, **106**, 11-19.
22. M. Kaveh, S. A. S., H. Jie, R. S. C. F. and A. R. P., *J. Biomed. Mater. Res., Part A*, 2015, **103**, 981-989.
23. C. Gabriel, W. B. C. and W. T. J., *J. Biomed. Mater. Res., Part A*, 2006, **78A**, 595-604.
24. T. Wang, J.-C. Zhang, Y. Chen, P.-G. Xiao and M.-S. Yang, *J. Trace Elem. Med. Biol.*, 2007, **21**, 84-91.
25. B. Sommer, M. Bickel, W. Hofstetter and A. Wetterwald, *Bone*, 1996, **19**, 371-380.
26. N. Garino, T. Limongi, B. Dumontel, M. Canta, L. Racca, M. Laurenti, M. Castellino, A. Casu, A. Falqui and V. Cauda, *Nanomaterials*, 2019, **9**, 212.
27. K. Ocakoglu, S. Mansour, S. Yildirimcan, A. A. Al-Ghamdi, F. El-Tantawy and F. Yakuphanoglu, *Spectrochim. Acta, Part A*, 2015, **148**, 362-368.
28. A. Sanginario, V. Cauda, A. Bonanno, K. Bejtka, S. Sapienza and D. Demarchi, *RSC Adv.*, 2016, **6**, 891-897.
29. B. Miccoli, V. Cauda, A. Bonanno, A. Sanginario, K. Bejtka, F. Bella, M. Fontana and D. Demarchi, *Sci. Rep.*, 2016, **6**, 29763.
30. G. N., L. A., G. R., C. A. and G. C., *J. Alloy Compd.* , 2014, **615**, S454-S458.
31. A. Ancona, B. Dumontel, N. Garino, B. Demarco, D. Chatzitheodoridou, W. Fazzini, H. Engelke and V. Cauda, *Nanomaterials*, 2018, **8**, 143.
32. N. Gómez-Cerezo, S. Sánchez-Salcedo, I. Izquierdo-Barba, D. Arcos and M. Vallet-Regí, *Acta Biomater.*, 2016, **44**, 73.
33. L. Racca, M. Canta, B. Dumontel, A. Ancona, T. Limongi, N. Garino, M. Laurenti, G. Canavese and V. Cauda, in *Smart Nanoparticles for Biomedicine*, ed. G. Ciofani, Elsevier, 2018, DOI: 10.1016/B978-0-12-814156-4.00012-4, ch. 12, pp. 171-187.
34. N. Encimas, M. Angulo, C. Astorga, M. Colilla, I. Izquierdo-Barba and M. Vallet-Regí, *Acta Biomater.*, 2019, **15**, 317.